EPJ Web of Conferences **126**, 02011 (2016) DOI: 10.1051/epjconf/201612602011
*ICNFP 2015*

# Recent Results of the CMS Experiment

Tommaso Dorigo[1a] on behalf of the CMS Collaboration

[1] *INFN - Sezione di Padova*

**Abstract.** The CMS experiment has produced a large number of new measurements with data collected during Run 1 by the CERN Large Hadron Collider (LHC). In this report a few results in Higgs and top physics will be mentioned. After a shutdown in 2013 and 2014, the LHC restarted proton-proton collisions at the unprecedented center-of-mass energy of 13 TeV in June 2015. The data collected until August 2015 have yielded interesting events and allowed the extraction of the first results of searches at the high-energy end of mass spectra, where the effect of the higher collision energy is largest.

## 1 Introduction

After the 2012 discovery[1] of the Englert-Brout-Higgs boson [2–7][1], a detailed investigation of the properties of that new particle has been carried out with all the data collected in Run 1 by the Large Hadron Collider. The observable characteristics of the Higgs boson as measured by the CMS experiment currently fit perfectly to the predictions of the standard model (SM). The mining of Run 1 data in imaginative new ways has paid dividends, with the extraction of several new bits of information; in particular, differential distributions of Higgs production properties have been for the first time extracted by the analysis of CMS data. A more precise determination of the Higgs boson couplings and a study of its less frequent decay modes are foreseen with the data that has started to be collected in June 2015 at 13 TeV center-of-mass energy.

In parallel with the careful study of the Higgs boson, a number of measurements of SM processes has been systematically carried out in Run 1 data. In this report we will only mention a couple of recent results in top quark physics. The reader is referred to the public pages of the CMS experiment for a complete list of all available measurements [8].

The search for new phenomena is of course today the main focus of the CMS experiment. While the studies of 7- and 8-TeV collisions have revealed no significant departures from SM predictions, the range of possible signals of new physics hiding in the huge datasets so far collected is quite broad, and surprises are still possible. A mention of the many results produced by those searches is impossible in this brief report; a summary can be found in the reports from the parallel sessions in these proceedings.

This document is organized as follows. Section 2 provides a brief description of the experiment. In Section 3 is offered a short review of the most interesting results of the investigations of the nature of the new 125 GeV scalar particle. Section 4 describes two recent top physics results using Run 1 data. In Section 5 are highlighted a few recent results from the analysis of the 13 TeV collisions produced by the Large Hadron Collider since June 2015 . Some conclusions are offered in Section 6.

[a] e-mail: dorigo@pd.infn.it

[1] In the following, for brevity we will address the particle simply as “Higgs boson”.

## 2 The CMS Detector and the Datasets

CMS –an acronym for Compact Muon Solenoid– is a multi-purpose magnetic detector designed to study the multi-TeV proton-proton collisions delivered by the CERN Large Hadron Collider. The detector is located in a underground cavern at a depth of 100m in Cessy, near the border of France and Switzerland. Particles emitted in hard collisions at the center of CMS cross in succession a silicon tracker, electromagnetic and hadron calorimeters, a solenoid magnet, and muon drift chambers embedded in the solenoid iron return yoke.

### 2.1 Overview of the CMS Detector

The momenta of charged particles emitted in the collisions at the center of the CMS detector are measured using a 13-layer silicon pixel and strip tracker; 66 million silicon pixels of dimensions 100x150 $\mu m$ are arranged in three barrel layers, and are surrounded by 9.6 million 180 $\mu m$-wide silicon strips arranged in additional concentric barrels in the central region and disks in the endcap region. In order to allow a precise measurement of charged particle momenta, the silicon tracker is immersed in the 3.8 T axial field produced by a superconducting solenoid. The tracker covers the pseudorapidity [2] range $|\eta| < 2.5$.

Surrounding the tracker are an electromagnetic calorimeter (ECAL) composed of lead tungstate crystals and a brass-scintillator hadron calorimeter (HCAL). These detectors are used to measure the energy of incident particles from the produced electromagnetic and hadronic cascades; they consist of a barrel assembly covering the central region, plus two endcaps covering the solid angle for particles emitted at lower angle with respect to the beams direction. The ECAL and HCAL cover the pseudorapidity range $|\eta| < 3.0$; at still smaller angles particles emitted in the collision encounter a steel/quartz-fiber Cherenkov forward detector (HF) which extends the calorimetric coverage to $|\eta| < 5.0$.

The outermost component of the CMS detector is the muon system, whose main component is a set of four layers of gas detectors placed within the steel return yoke. The muon system performs a high-purity identification of muon candidates and a stand-alone measurement of their momentum, and in combination with the inner tracker information it provides a high-resolution determination of muon kinematics. More detail on the CMS detector is provided elsewhere [9].

CMS collects data with a two-level trigger system. Level 1 is a hardware trigger based on custom-made electronic processors that receive as input a coarse readout of the calorimeters and muon detectors and perform a preliminary selection of the most interesting events for data analysis, with an output rate of about 100 kHz. Level 2, also called "High-Level Trigger" (HLT), uses fine-grained information from all sub-detectors in the regions of interest identified by Level 1 to produce a final decision, selecting events at a rate of about 300 Hz by means of speed-optimized software algorithms running on commercial computers.

### 2.2 Run 1 and Run 2

Many of the results discussed in the following sections are based on the full data samples collected in 2011 and 2012, a period referred to as Run 1. The 2011 proton-proton run of the LHC produced collisions at the center-of-mass energy of 7 TeV. In the course of seven months of data taking CMS acquired a total of 5.3 inverse femtobarns of integrated luminosity; 5.0 of these were collected with all the CMS subdetectors fully operational. In 2012 the LHC has been operating at the increased energy

[2] Pseudorapidity is defined as $\eta = -ln \tan \theta/2$, where $\theta$ is the polar angle of the particle trajectory with respect to the direction of the counter-clockwise proton beam.

of 4 TeV per beam; in total, CMS acquired a total of 21.8 inverse femtobarns of proton-proton collisions at a center-of-mass energy of 8 TeV. The LHC in 2012 ran at higher instantaneous luminosities than in 2011; this produced a high pileup of 20 to 50 simultaneous interactions per bunch crossing. CMS addressed the resulting reconstruction challenge with more sophisticated algorithms and calibration procedures, which have allowed to maintain the same physics output despite the harsher experimental conditions.

During the post-Run1 shutdown CMS prepared for Run 2 in several ways. The main challenge was to mitigate the effects of radiation on the performance of the tracker. This was mainly addressed by preparing the detector for operation at low temperatures (down to $-20^o$C). The cooling plant and distribution were modified to prevent condensation. The central beampipe was also replaced by a narrower one in preparation for the installation, in 2016-17, of a new Pixel Tracker that will better measure the momenta and points of origin of charged particles. In the muon system, a fourth measuring station was added to each muon endcap in order to maintain discrimination between low-momentum muons and background as the LHC beam intensities increase. This was complemented by two 125-ton shielding structures at each end of detector, reducing neutron backgrounds. A better luminosity measurement is granted by a luminosity-measuring device, the Pixel Luminosity Telescope, which was installed on either side of the collision point around the beam pipe. Other improvements include the replacement of photo-detectors in the hadron calorimeter with better-performing designs and the moving of the muon readout to more accessible locations for maintenance. A first stage of a new hardware triggering system was also installed. Finally, the software and computing systems underwent a significant overhaul during the shutdown, to reduce the time needed to produce analysis datasets.

Run 2, started in June 2015, delivered proton-proton collisions to the experiments at the center-of-mass energy of 13 TeV. The data taking in 2015 was divided in a first period when proton bunches were separated by 50 ns as in Run 1, and a longer period of collisions with 25 ns spaced bunches. The shorter bunch spacing reduced the effect of pileup. A few preliminary results produced with 2015 data collected in June and July is discussed in Section 5.

## 3 Recent Results in Higgs Boson Physics

Due to its non-zero coupling to all massive particles, the Higgs boson can be produced through several different mechanisms in proton-proton collisions. CMS has studied all the dominant production processes: ones due to gluon-fusion diagrams, where a Higgs boson is emitted by a virtual top-quark or vector boson loop; vector-boson-fusion processes, where the Higgs is produced together with two high-rapidity hadronic jets that result from the emission of virtual W or Z bosons off the initial state quarks; and Higgs-strahlung diagrams, where the particle is radiated by a highly-off-shell W or Z boson or by a top quark.

The Higgs boson also exhibits a rich decay phenomenology. The decays to weak boson pairs ($H \to WW^*$, $H \to ZZ^*$) are possible when one of the two final-state objects is off-mass-shell: their branching ratios are comparatively small, which allows other decays to be observable. CMS has so far obtained significant signals from five different decay modes of the Higgs boson: the two mentioned above, as well as decays to b-quark pairs, $\tau$-lepton pairs, and photon pairs. The latter, although quite rare (with a branching fraction of $2.3\times10^{-3}$ in the SM), has in fact been crucial for the first observation of the Higgs boson. Other rare decay modes (*e.g.* $H \to Z\gamma$, $H \to \mu\mu$) will also become accessible to a direct measurement in the future.

Among all Higgs boson properties measured by CMS in Run 1, in this brief report we single out the Higgs mass. Thanks to very careful measurements exploiting both in the $ZZ$ and the $\gamma\gamma$ decay modes,

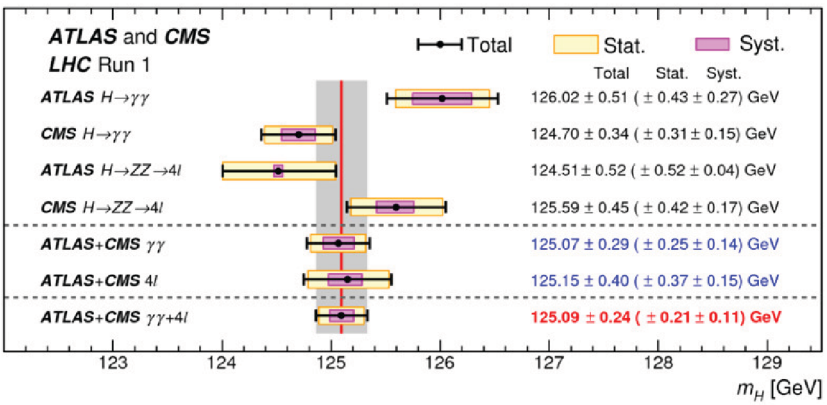


**Figure 1.** *Measurements of the Higgs boson mass by ATLAS and CMS in the diphoton and ZZ final states, and their combination.*

the Higgs boson mass is determined by CMS to be $M_H = 125.02 \pm 0.27 \pm 0.15$ GeV. Once combined with slightly less precise ATLAS results, the best estimate [10] is $M_H = 125.09 \pm 0.21 \pm 0.11$ GeV; in both the measurements quoted above the first uncertainty is statistical and the second includes all systematic effects. Figure 1 shows the four independent determinations by the LHC experiments and their combination results.

One recent result is worth mentioning here. Higgs boson decay candidates have been used to study differential cross sections of Higgs production in a fiducial region of the event kinematics [11]. The restriction of the measurement to a region of phase space matching the detector acceptance reduces model systematics. Cross sections have been derived in the fiducial volume at 7 and 8 TeV independently, by maximum likelihood fits to the data assuming a Higgs boson mass $M_H = 125$ GeV. The results are compared to predictions at next-to-next-to-leading order (NNLO) plus next-to-next-to-leading-logarithm (NNLL) from several generators [12–16].

Besides the cross section at 7 and 8 TeV, the considered variables for differential production cross section studies are the transverse momentum and rapidity of the four leptons in $H \to ZZ^* \to 4l$ decays, and the kinematics of the Higgs boson with respect to the leading jet. Results match nicely the precise theoretical predictions at NNLO in all considered distributions. Figure 2 (left) shows for example the measured Higgs boson cross section versus Higgs transverse momentum.

Higgs bosons have also started to be used in searches for new physics, by considering resonances that may decay to Higgs boson pairs. One example [17] is the study of models inspired by warped extra dimensions, which predict the existence of spin-0 Radions $X$, or spin-2 Kaluza-Klein excitations of the graviton. Due to small cross sections of the predicted phenomena, the only practical Higgs decay mode to exploit in these searches is currently the $H \to b\bar{b}$ one. Searches for resonant $X \to HH$ production and decay to $b\bar{b}b\bar{b}$ final states have been performed by CMS in the non-boosted regime ($M_X < 1$ TeV). Decays of heavy objects into HH pairs result in highly boosted b-quark jets that at detector level merge in a single observed "fat jet". These topologies can now be spotted and separated from backgrounds using jet substructure techniques. In particular, the two-subjet mass can be effectively used to distinguish H decays from generic jets. B-tagging is also used to reduce the irreducible QCD background: secondary vertices are sought in the sub-jets, or in the fat jet if the

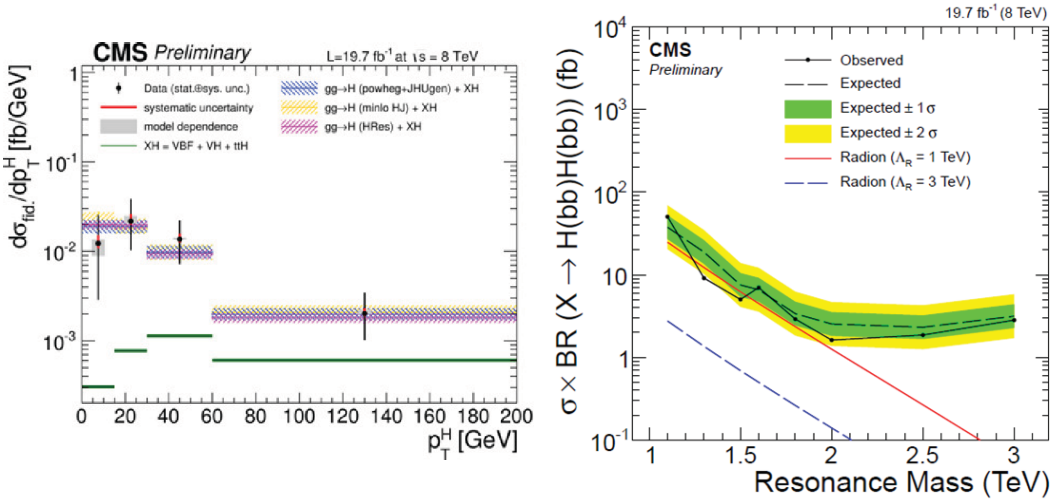


**Figure 2.** *Left: differential cross section of Higgs boson production as a function of Higgs transverse momentum. The data (black points with vertical bars) is compared with the predictions of several generators. The green histogram shows the predicted contribution from vector-boson-fusion and associated production processes. Right: upper limit on the product of Radion cross section times branching fraction into two Higgs bosons, with subsequent decays to bottom-quark pairs.*

sub-jets are at a radial distance $\Delta R < 0.3$ in pseudorapidity-azimuth space. B-tagged jets with mass in the 110-135 GeV range are called "H-jets". Events are retained if both jets are H-jets, and at least one of the two leading jets is b-tagged using the tight working point of the CSV algorithm (both subjets are tagged, or the fat jet is).

To further reduce backgrounds, the $\tau_{21}$ variable, describing the two-component substructure of the jet, is used to separate H-jets into a "high-purity" (HP) and a "low-purity" (LP) category. Three event categories are then created, depending on the above classification of the candidates: HP-HP, HP-LP, and LP-LP. A data-driven fit cross-checked in control samples and MC is used to extract the signal contribution and set upper limits. Figure 2 (right) shows the combined limit on Radion cross section from the combination of the search performed in the three categories.

## 4 Top Quark Physics

CMS produced many groundbreaking results in top quark physics with Run 1 data. Here we only mention the determination of the mass of the top quark, which is a very important parameter in the SM due to its impact in global electroweak fits and its effect on the predicted meta-stability of the Higgs boson potential. The combination of CMS measurements of the top mass [25] yields $M_t = 172.44 \pm 0.13 \pm 0.47$ GeV, where the first uncertainty is statistical and the second includes all systematic uncertainties. This result is the most precise to date. The CMS determination presents a small tension with the Tevatron average [24] ($M_t = 174.34 \pm 0.37 \pm 0.52$ GeV), mostly due to the high determination produced by the DZERO experiment. A summary of recent top mass determinations and combinations by CMS is given in Fig. 3 (left).

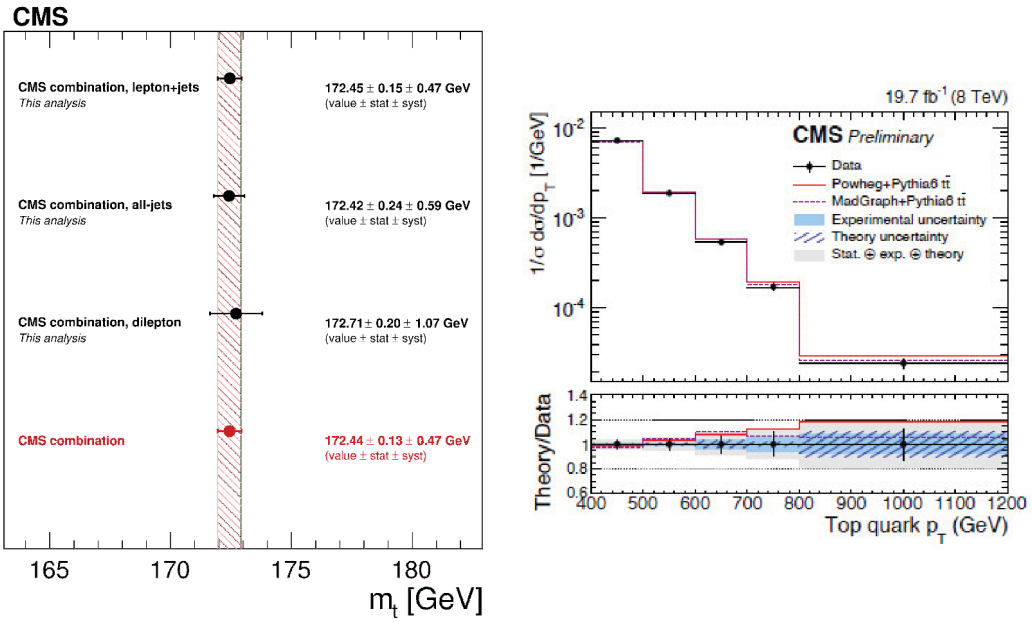


**Figure 3.** *Left: recent measurements of the top quark mass by the CMS experiment in the three main decay channels, and their global combination. Right: top quark $p_T$ distribution measured by CMS with boosted objects identification techniques, compared to predictions of the Powheg generator.*

While the integrated top production cross section has been measured using all main final states and is now in the realm of precision measurements, its determination at high top-quark $p_T$ may still offer ground for potential surprises. The high-end tail of the top quark $p_T$ distribution has been measured by CMS [18] by searching for "boosted tops": the top quark decay products merge together as b-decay products do, creating a wide jet where substructure techniques can identify the decay and allow a reconstruction of the mass.

The boosted top technique works for $p_T > 400$ GeV, a complementary regime to the one studied with non-boosted top identification methods. A wide Cambridge-Aachen jet (CA8) is the input of the CMS hadronic top tagging algorithm in the boosted regime. This requires the presence of three subjets with all jet-pair masses above 50 GeV and a three-body-mass in the 140-250 GeV range. Opposite to the hadronic boosted top, the other top quark is required to undergo a leptonic decay. There, a regular anti-$k_T$ (AK5) jet is used, accompanied with a lepton and neutrino signature.

A fit extracts the top pair-production signal from four independent categories of events, divided by the presence of an electron or muon in the leptonic top side and by the presence of a b-tag in the lepton-side jet. The $p_T$ distribution of the QCD background is modeled with a data-driven technique based on a fit to the missing transverse energy distribution to obtain the normalization, plus a shape determined in a signal-poor control sample. Other backgrounds from single top and W+jets production are determined from Monte Carlo simulations. SVD unfolding is used to extract the particle-level $p_T$ distribution of the signal component. The resulting spectrum shows a slight deficit at high $p_T$ with respect to Powheg predictions (see Fig. 3, right).

## 5 A First Look at Run 2 Data

The first Run 2 data was used by CMS to verify the operational status of all detector components, checking the event reconstruction and the resolution on energy and momentum measurements using known particle signals. All the while, the highest-energy events were scrutinized carefully, as the 62.5% increase in center-of-mass energy grants large cross-section enhancements for high-mass resonances, particularly ones produced by gluon-initiated processes. Figure 4 shows an event display of an early 1-TeV dielectron event (left), and a spectacular dijet event with a jet-jet mass of 5.4 TeV (right).

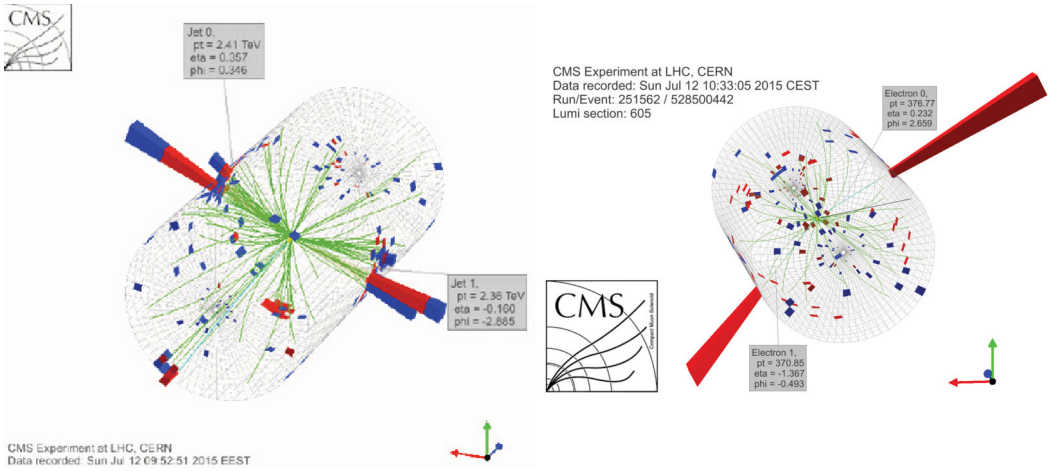


**Figure 4.** *Left: three-dimensional view of the energy deposits left by a high-energy dijet event collected in Run 2. The combined mass of the two leading jets is of 5.4 TeV. Right: a dielectron event with total invariant mass of 1 TeV.*

One of the first quantitative results extracted from the new data is the top pair-production cross section at 13 TeV. This measurement uses $42 pb^{-1}$ of dilepton candidates in the $e\mu$ +jets final state, collected by a trigger selecting events with high-momentum electron-muon pairs. Offline, events are selected if leptons have $p_T > 20$ GeV and $|\eta| < 2.4$, and isolated from hadronic activity. Anti-$k_T$-clustered jets are counted if they have $p_T > 30$ GeV and $|\eta| < 2.4$. The event selection includes a requirement of at least two jets with those characteristics.

The signal is modeled with the Powheg 2.0 NLO generator interfaced with Pythia 6 for hadronization. The signal to noise ratio for events with two or more jets is already good enough that no b-tagging is necessary to further reduce backgrounds. Systematic uncertainties in the measurement include the knowledge of integrated luminosity (12%, from beam-beam scans), trigger (5%) and lepton identification (4%), and jet energy scale (3%). The $t\bar{t}$ cross section is extracted from the event counts, once backgrounds are accounted for. The result is $\sigma_{t\bar{t}} = 772 \pm 60(stat) \pm 62(syst) \pm 93(lumi)$ pb, with a total relative uncertainty of 13.5%. This measurement is consistent with the SM prediction ($\sigma_{NNLO+NNLL}(t\bar{t}) = 832^{+40}_{-46}$ pb), valid for a top quark mass of 172.5 GeV. Figure 5 compares the 13 TeV measurement with previous ones and with theory predictions as a function of the center-of-mass energy of the collisions.

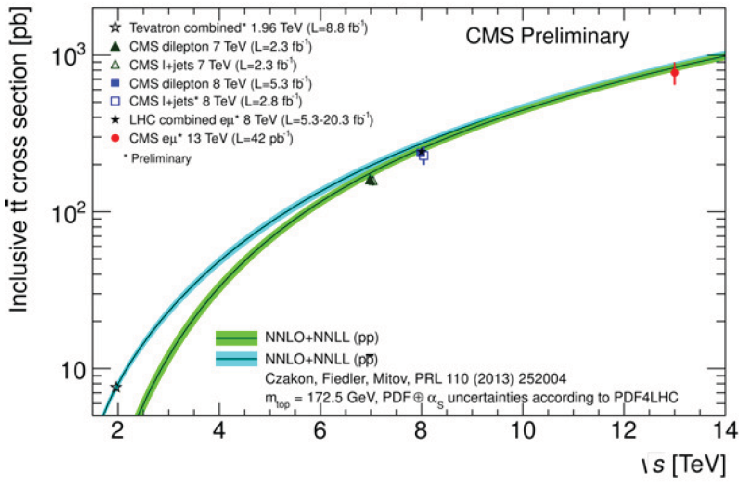


**Figure 5.** *Determinations of the top pair-production cross section in hadron-hadron collisions as a function of the center-of-mass energy. The recent CMS determination at 13 TeV is shown by the red marker on the right.*

## 6 Conclusions

The CMS experiment has exploited proton-proton collision data collected during the 2011 and 2012 runs of the Large Hadron Collider to produce a large number of groundbreaking results in precision measurements of SM observables and searches for new physics. The most recent results include differential distributions of Higgs boson production, top quark measurements at high transverse momentum, and much more. CMS also produced the most precise measurements to date of the mass of the top quark and of the Higgs boson.

The first data collected in the summer of 2015 have allowed the experiment to tune its detector components and reconstruction algorithms, and to start producing new measurements at the so far untested collision energy of 13 TeV. The measurement of top quark pair-production cross section is in excellent agreement with theoretical predictions. Events at the high-energy end of mass spectra have already started to inspire hopes that the new energy regime will provide hints of new physics.

## Acknowledgements

We wish to congratulate our colleagues in the CERN accelerator departments for the excellent performance of the LHC machine. We thank the technical and administrative staff at CERN and other CMS institutes, and acknowledge support from: FMSR (Austria); FNRS and FWO (Belgium); Cap, CAPES, FAPERJ, and FAPESP (Brazil); MES (Bulgaria); CERN; CAS, Most, and NSFC (China); COLCIENCIAS (Colombia); MSES (Croatia); RPF (Cyprus); More, SF0690030s09 and ERDF (Estonia); Academy of Finland, MEC, and HIP (Finland); CEA and CNRS/IN2P3 (France); BMBF, DFG, and HGF (Germany); GSRT (Greece); OTKA and NKTH (Hungary); DAE and DST (India); IPM (Iran); SFI (Ireland); INFN (Italy); NRF and WCU (Korea); LAS (Lithuania); CINVESTAV, CONACYT, SEP, and UASLPFAI (Mexico); MSI (New Zealand); PAEC (Pakistan); MSHE and NSC (Poland); FCT (Portugal); JINR (Armenia, Belarus, Georgia, Ukraine, Uzbekistan); MON, Rosa tom, RAS and RFBR (Russia); MSTD (Serbia); MICINN and CPAN (Spain); Swiss Funding Agencies (Switzerland); NSC (Taipei); TUBITAK and TAEK (Turkey); STFC (United Kingdom); DOE and NSF (USA).

## References

[1] CMS Collaboration, *Observation of a new boson at a mass of 125 GeV with the CMS experiment at the LHC*, Phys. Lett. **B716** (2012) 30-61; ATLAS Collaboration, *Observation of a new particle in the search for the standard model Higgs boson with the ATLAS detector at the LHC*, Phys. Lett. **B716** (2012) 1.

[2] F. Englert and R. Brout, *Broken symmetry and the mass of gauge vector mesons*, Phys. Rev. Lett. **13** (1964) 321-323.

[3] P. Higgs, *Broken symmetries, massless particles and gauge fields*, Phys. Lett. **12** (1964)132-133.

[4] P. Higgs, *Broken symmetries and the masses of gauge bosons*, Phys. Rev. Lett. **13** (1964) 508-509.

[5] G. Guralnik, C. Hagen, and T. Kibble, *Global conservation laws and massless particles*, Phys. Rev. Lett. **13** (1964) 585-587.

[6] P. Higgs, *Spontaneous symmetry breakdown without massless bosons*, Phys. Rev. **145** (1966) 1156-1163.

[7] T. Kibble, *Symmetry breaking in non-Abelian gauge theories*, Phys. Rev. **155** (1967) 1554-1561.

[8] See http://cms-results.web.cern.ch/cms-results/public-results/publications/.

[9] CMS Collaboration, *The CMS experiment at the CERN LHC*, J.Instrum. **3** (2008) S08004.

[10] CMS Collaboration, *Combined measurement of the Higgs boson mass in pp collisions at* $\sqrt{s} = 7$ *and* 8 *TeV with the ATLAS and CMS experiments*, Phys. Rev. Lett. **114** (2015) 191803.

[11] CMS Collaboration, *Measurement of inclusive and differential fiducial cross sections for Higgs boson production in the* $H \to 4l$ *decay channel in p-p collisions at* $\sqrt{s} = 7$ *and* $\sqrt{s} = 8$ *TeV*, CMS-PAS-HIG-14-028, arXiv:1512.08377 (2015).

[12] D. de Florian, G. Ferrera, M. Grazzini, and D. Tommasini, *Higgs boson production at the LHC: transverse momentum resummation effects in the* $H \to \gamma\gamma$, $H \to WW \to l\nu l\nu$ *and* $H \to ZZ \to 4l$ *decay modes*, J. High Energy Phys. **06** (2012) 132, doi:10.1007/JHEP06(2012)132, arXiv:1203.6321 (2012).

[13] M. Grazzini and H. Sargsyan, *Heavy-quark mass effects in Higgs boson production at the LHC*, J. High Energy Phys. **09** (2013) 129, doi:10.1007/JHEP09(2013)129, arXiv:1306.4581 (2013).

[14] S. Frixione, P. Nason, and C. Oleari, *Matching NLO QCD computations with parton shower simulations: the POWHEG method*, J. High Energy Phys. **11** (2007) 070, doi:10.1088/1126-6708/2007/11/070, arXiv:0709.2092 (2007).

[15] T. Melia, P. Nason, R. Rontsch, and G. Zanderighi, *W+W-, WZ and ZZ production in the POWHEG BOX*, J. High Energy Phys. **11** (2011) 078, doi:10.1007/JHEP11(2011)078, arXiv:1107.5051 (2011).

[16] K. Hamilton, P. Nason, and G. Zanderighi, *MINLO: multi-scale improved NLO*, J. High Energy Phys. **10** (2012) 155, doi:10.1007/JHEP10(2012)155, arXiv:1206.3572 (2012).

[17] CMS Collaboration, *Search for resonant pair production of Higgs bosons decaying to two bottom quark-antiquark pairs in proton-proton collisions at 8 TeV*, Phys. Lett. **B749** (2015) 560.

[18] CMS Collaboration, *Measurement of the differential $t\bar{t}$ production cross section for high-$p_T$ top quarks in $e\mu$+jets final states at 8 TeV*, CMS-PAS-TOP-14-012 (2014).

[19] CMS Collaboration, *Measurement of the $t\bar{t}$ production cross section in the dilepton channel in pp collisions at $\sqrt{s}$ = 7 TeV*, J. High Energy Phys. **11** (2012) 067.

[20] CMS Collaboration, *Measurement of the $t\bar{t}$ production cross section in the dilepton channel in pp collisions at $\sqrt{s}$ = 8 TeV*, CMS-PAS-TOP-12-007, axXiv:1312.7582 (2013).

[21] M. Campbell and R. K. Ellis, *MCFM for the Tevatron and the LHC*, Nucl. Phys. Proc. Suppl. **205-206** (2010) 10, arXiv:1007.3492 (2010).

[22] M. Aliev et al., *HATHOR: HAdronic Top and Heavy quarks crOss section calculatoR*, Comput. Phys. Commun. **182** (2011) 1034.

[23] N. Kidonakis, *Next-to-next-to-leading soft-gluon corrections for the top quark cross section and transverse momentum distribution*, Phys. Rev. **D82** (2010) 114030.

[24] Tevatron Electroweak Working Group, *Combination of the CDF and D0 results on the mass of the top quark using up to 9.7 $fb^{-1}$ at the Tevatron*, arXiv:1407.2682 (2014).

[25] CMS Collaboration, *Measurement of the top quark mass using proton-proton data at $\sqrt{s}$ = 7 and 8 TeV*, arXiv:1509.04044, CMS-PAS-PUB-14-022 (2015), accepted for publication in Phys. Rev. D.